Dielectric behavior at the smectic-C^*–chiral-nematic phase transition of a ferroelectric liquid crystal

S. Hiller, A. M. Biradar,* S. Wrobel,† and W. Haase
Institut für Physikalische Chemie, Technische Hochschule Darmstadt, Petersenstrasse 20, 64287 Darmstadt, Federal Republic of Germany
(Received 23 May 1995)

The dielectric relaxation processes of a ferroelectric liquid crystal material with a first order phase transition (chiral-nematic to smectic-C^*) have been investigated using thin, gold coated electrode cells in the frequency range of 10 Hz to 13 MHz. The results have been reported for planar and homeotropic aligned cells. The surfaces of the electrode cells were not given any surface treatment for alignment in order to minimize the surface anchoring effect on the dielectric processes. The orientation was done by a magnetic field. It has been observed that in planar alignment three dielectric collective processes, namely, the Goldstone mode, domain mode, and soft mode, connected to the director reorientation were detected. The soft mode process obeys the Curie-Weiss law at the temperature of the Sm-C^* to N^* phase transition. In homeotropic alignment the molecular relaxation around the short axis of the molecule has been observed in the N^* phase. The results have been discussed in view of temperature dependences of the different dielectric processes in planar alignment with respect to the relaxation frequency and dielectric strength in the smectic-C^* and chiral-nematic phases. For homeotropic alignment it is reported in the N^* phase only.

PACS number(s): 61.30.-v, 77.20.+, 77.40.+i

I. INTRODUCTION

In recent years considerable theoretical and experimental work has been devoted to the study of the dielectric response of ferroelectric liquid crystals (FLC's) with a phase sequence of smectic-A to smectic-C^* transition [1-4]. FLC materials showing a chiral nematic (N^*) to smectic-C^* (Sm-C^*) phase transition have been scarcely studied so far [5] because of the difficulty in obtaining well-aligned cells. However, these FLC's are very interesting for practical applications, since their material constants, such as tilt angle, are as large as 45°, do not depend greatly on temperature, and can be better suited for preparing electro-optical switches [6] and guest-host displays [7].

It is known that the dielectric permittivity in chiral-smectic phases is first due to the collective dielectric processes, connected with the director reorientational motion, and second to the molecular reorientation motion, connected with the dipolar polarizability of the molecule. The collective dielectric processes are due to the Goldstone mode, connected to the change of the direction of the tilt of the molecules, and the soft mode which is due to the change of the magnitude of the tilt of the molecules. The other collective dielectric process is due to the domain mode [8], which is generally observed with high-spontaneous-polarization (P_s) FLC materials. The molecular reorientation processes around the long and short axes of the molecule are present in all the liquid crystalline phases, and can be measured, depending upon whether the measuring electric field is perpendicular or parallel to the director [9].

The director relaxation can be described in terms of the complex dielectric permittivity, which is given as

$$\varepsilon^*(\omega,T)=\varepsilon'(\omega,T)-i\varepsilon''(\omega,T)\ , \tag{1}$$

where ε' gives the real part of the dielectric permittivity, and its spectrum is called the dispersion curve. ε'' gives the imaginary part of the complex permittivity, and its spectrum is called the absorption (or dielectric loss) curve. ω is the angular frequency of the applied electric field, and T is the temperature of the system. In order to characterize the temperature dependence of the observed dielectric relaxation, $\varepsilon^*(\omega)$ can be described by Debye formulas as follows:

$$\varepsilon'(\omega,T)=\varepsilon_\infty+\frac{\varepsilon_0(T)-\varepsilon_\infty}{1+\omega^2\tau(T)^2} \tag{2}$$

and

$$\varepsilon''(\omega,T)=\frac{[\varepsilon_0(T)-\varepsilon_\infty]\omega\tau(T)}{1+\omega^2\tau(T)^2}\ , \tag{3}$$

where ε_0 is the static dielectric permittivity, ε_∞ is the high frequency limit of the electric permittivity, and τ is the relaxation time. The generalization of the Debye formulation describes a dielectric process with a discrete distribution of relaxation times associated with a single dielectric process. However, if a dielectric process exhibits a continuous distribution of the relaxation time, it can be described by the Cole-Cole function as

*Permanent address: National Physical Laboratory, Dr. K.S. Krishnan Road, New Delhi 11012, India.
†Permanent address: Institute of Physics, Jagellonian University, Reymonta 4, 30-059 Krakow, Poland.

$$\varepsilon^*(\omega)=\varepsilon_\infty+\frac{\varepsilon_0-\varepsilon_\infty}{1+(i\omega\tau)^{1-\alpha}}\ , \tag{4}$$

where α is the distribution parameter for a particular relaxation process. Using the Havriliak-Negami function, where the asymmetry of the absorption curve is considered (via parameter β), a dielectric spectrum can be described by

$$\varepsilon^*(\omega)=\varepsilon_\infty+\frac{\varepsilon_0-\varepsilon_\infty}{[1+(i\omega\tau)^{1-\alpha}]^\beta}\ . \tag{5}$$

In this paper, we report on investigations of different dielectric relaxation processes in planar ($\varepsilon_\perp$) and homeotropically ($\varepsilon_\parallel$) aligned cells of a single component ferroelectric liquid crystal material which shows a first order phase transition having a phase sequence of chiral-nematic to smectic-C^* phases with high-spontaneous-polarization values. It has been found that collective dielectric processes such as the Goldstone mode, soft mode, and domain mode are present in the Sm-C^* phase. Up to 4–5 K above T_c temperature (the transition temperature of the Sm-C^* to N^* phases) the soft mode is observed for the N^* phase in planarly aligned cell. The molecular relaxation around the short axis is observed for the N^* phase in homeotropic alignment. The influence of the biasing field on collective dielectric processes was studied in detail in the Sm-C^* phase and close to T_c. The temperature dependences of different dielectric processes in both alignment configurations have also been reported and discussed.

II. EXPERIMENT

In order to minimize the surface anchoring effect, no surface treatment was done for the alignment. Gold coated electrode cells of different thicknesses were used. It was established that the planar and homeotropic alignment was better for thin cells. Indium tin oxide (ITO) electrodes were also used to check the alignment optically. Due to the high resistance of the ITO coating, this type of cell was not suitable for high-frequency measurements. To cover dielectric studies in the frequency range of 10 Hz to 13 MHz, highly conducting gold coated electrode cells were used.

Dielectric measurements were done in a shielded parallel-plate condensor [10]. The distance between the plates was kept around 3.5 μm by means of a mylar spacer for both configurations. The cells were first calibrated using air and toluene as standard references, which allowed us to calculate the absolute values of the electric permittivity. The single component ferroelectric liquid crystal material 3-octyloxy-6-[2-fluoro-4-(2-fluoro-octyloxy)phenyl]-pyridine (FFP) (IS-4362, E. Merck, Darmstadt, Germany) used in this investigation has the following phase diagram and phase sequence:

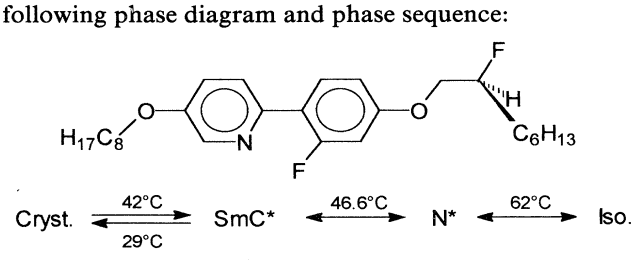

The FLC material was introduced into the cell by means of the capillary action in its isotropic phase. The planar and homoeotropic alignment of the FLC cell was obtained by putting the sample into a magnetic field of 1.2 T and cooling it slowly at the rate of 5 K/h from chiral-nematic to smectic-C^* phases (a few degrees below the transition temperature). The temperature of the sample was controlled with a heating system, and can be stabilized to an accuracy of 0.01 K. The cooling and heating cycles were performed several times to obtain a better alignment. The detail procedure of alignment by magnetic field is given elsewhere [4].

The dielectric measurements were done using a Hewlett-Packard impedance analyzer (HP 4192 A), controlled by a modified Atari Mega ST2 computer in the frequency range of 10 Hz to 13 MHz in planar and homeotropically aligned cells. The measurements were fully automated. The data were corrected for the static conductivity and for the high-frequency deviations caused by the inductance and resistance of the cables and connectors. The temperature, frequency, and bias field (generated by the impedance analyzer) dependences of the real and imaginary parts of the complex electric permittivity have been studied in Sm-C^* and N^* phases for both alignments.

III. RESULTS AND DISCUSSION

In this paper we discuss the dielectric relaxation processes in a single component ferroelectric liquid crystal material which shows a first order phase transition with a phase sequence of smectic-C^* to the chiral-nematic phase. Preliminary dielectric measurements for this material have been reported elsewhere [11] in an ITO-coated cell of planar alignment, which was done in surface treated samples in the presence of an electric field. The temperature and frequency dependences of the principal components of the complex electric permittivity in the planar alignment ($\varepsilon_\perp$) (where the measuring field is perpendicular to the director) and in the homeotropic alignment ($\varepsilon_\parallel$) (where the measuring field is parallel to the director) have been studied in Sm-C^* and N^* phases.

A. $\varepsilon_\perp$ component of complex electric permitivity

1. Goldstone mode in the Sm-C^* phase

It is well known that the $\varepsilon_\perp$ electric permittivity in the Sm-C^* phase is dominant at low frequencies due to the Goldstone mode contribution which comes from the phase fluctuations in the azimuthal orientation of the director. The dielectric spectrum due to the Goldstone mode is shown [Fig. 1(a)] in the form of dispersion and absorption curves as well as the Cole-Cole diagram [Fig. 1(b)]. The fitting to the experimental points was done with a Cole-Cole modification [Eq. (4)] of the Debye equation, and dielectric parameters such as the relaxation frequency, dielectric strength, and distribution parameter of the Goldstone mode were computed as given in the Table I. It is clear from the figure and table that the elec-

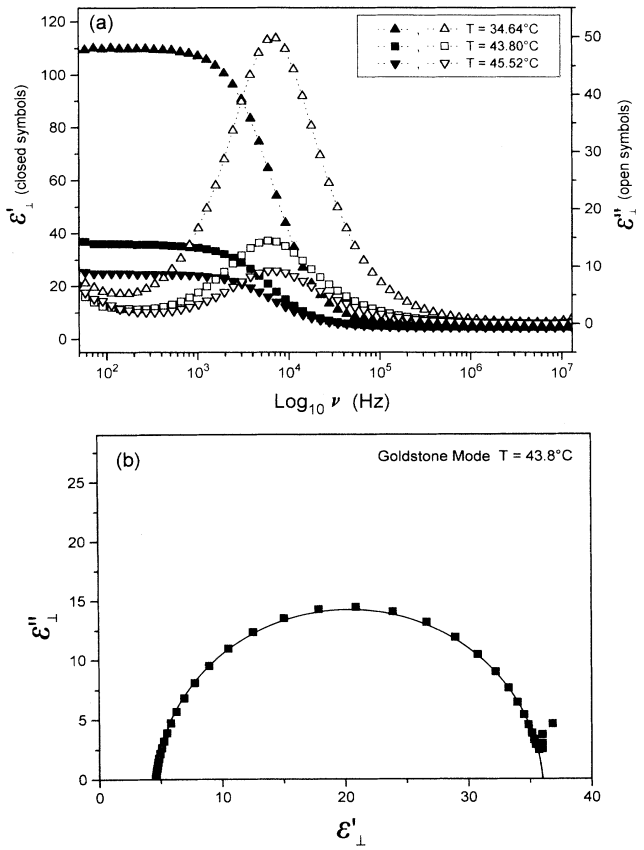

FIG. 1. (a) Dispersion (closed symbols) and absorption curves (open symbols) for Goldstone mode at different temperatures. (b) Cole-Cole representation of the Goldstone mode in the Sm-C^* phase.

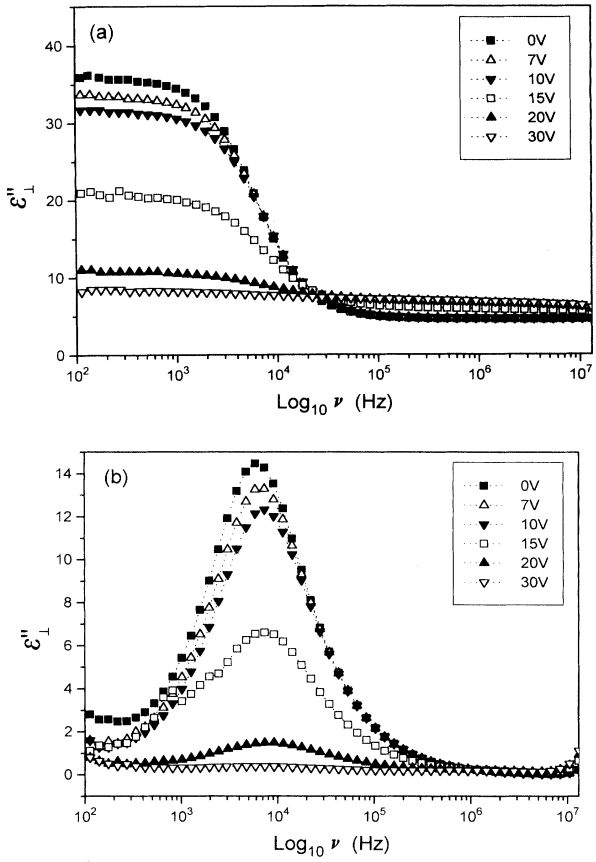

FIG. 2. Effect of biasing voltages on Goldstone mode at 43.8 °C temperature (a) dispersion and (b) absorption curves. Dotted lines are the fit curves of the Cole-Cole equations.

tric permittivity decreases near the transition temperature, whereas the relaxation frequency of the Goldstone mode is almost independent of temperature in the Sm-C^* phase [4].

The dielectric permittivity is very high in the Sm-C^* phase due to the Goldstone mode contribution, so it becomes difficult to detect the other collective dielectric processes, for instance the domain mode. However, this problem can be overcome by applying a dc bias field, being strong enough to unwind the helicoidal structure and suppress the Goldstone mode. In such a case one can study other collective processes such as the soft mode and domain mode. Figures 2(a) and 2(b) show the effect of bias voltage on the Goldstone mode in the form of dispersion and absorption curves. As the biasing voltage increases, the Goldstone mode contribution is suppressed. At about 20 V bias the electric permittivity and absorption of this mode are almost at a minimum. This means that this voltage is sufficient to unwind the helical structure of the system and suppress the contribution of the Goldstone mode. Figures 3(a) and 3(b) show the bias voltage dependence of the dielectric strength, relaxation frequency, and distribution parameter of the Goldstone mode. In particular, the drastic increase in the distribution parameter α [Fig. 3(b)] also suggests that above 15 V bias the Goldstone mode is suppressed, and one can observe the other collective dielectric processes in the Sm-C^* phase.

2. *Domain mode in Sm-C* phase*

As seen from Fig. 3, above 15 V biasing the Goldstone mode is suppressed, and one is able to see the other col-

TABLE I. Dielectric parameters of the Goldstone mode and the domain mode.

t (°C)	$\Delta\varepsilon_G$	ν_C^G(kHz)	α_G	$\Delta\varepsilon_D$	ν_C^D (kHz)	α_D
34.64	99.9	6.675	0.054	16.91	8.832	0.091
37.64	98.5	6.835	0.054	16.07	8.975	0.126
39.64	96.4	6.777	0.057	11.32	8.976	0.164
41.64	95.6	6.451	0.046	5.87	9.068	0.213
43.80	29.8	6.190	0.073	2.95	7.903	0.321
45.52	18.3	6.766	0.100	1.63	6.471	0.417

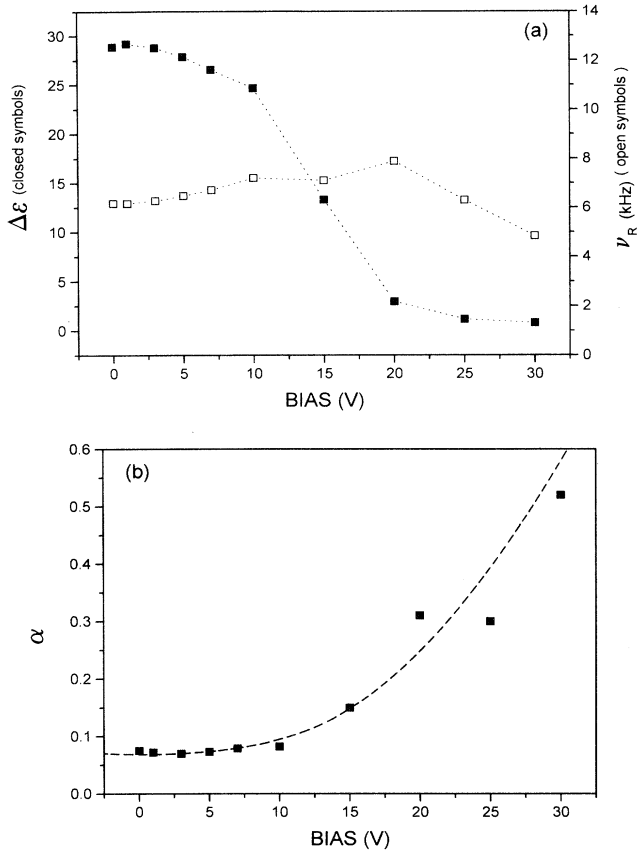

FIG. 3. (a) dc bias voltage dependence of the dielectric strength ($\Delta\varepsilon$) (closed squares) and relaxation frequency (ν_R) (open squares) of the Goldstone mode and (b) distribution parameter α of the Goldstone mode relaxation vs bias voltage at 43.8 °C temperature.

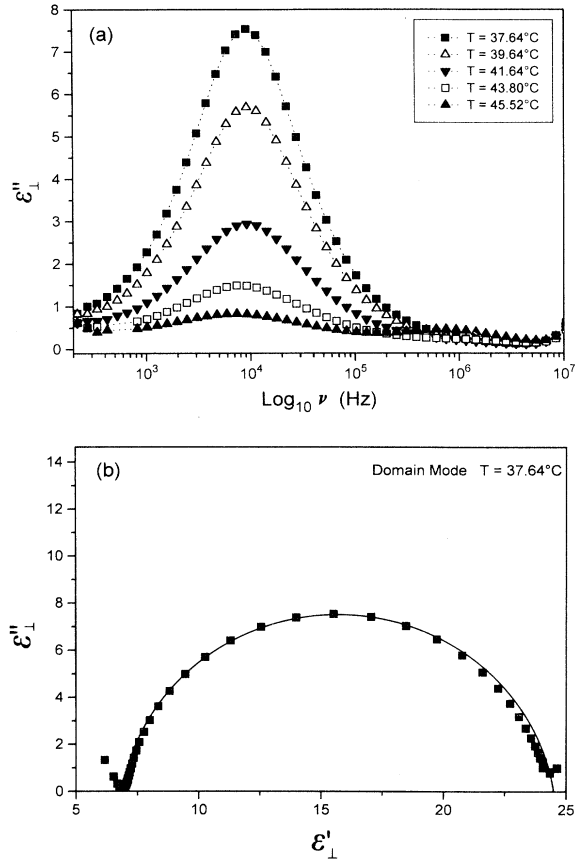

FIG. 4. (a) Dielectric spectra (imaginary part, i.e., $\varepsilon_\perp''$ vs frequency) of the domain mode for different temperatures in the Sm-C^* phase at 20-V biasing voltage (dotted lines are the fitting curves). (b) Cole-Cole plot for the domain mode process.

lective dielectric processes in the Sm-C^* phase. Recently it has been observed [8,12] that in FLC materials with considerably high spontaneous polarization ($P_s > 50$ nC/cm^2), and in the absence of helical structure, the symmetry breaks up into a special periodical structure to reduce the electrostatic energy, resulting in the formation of domains, which was considered to be an analog of solid ferroelectric domains. In the presently investigated FLC material, which has a very high spontaneous polarization ($P_s = 170$ nC/cm^2 at room temperature), the characteristic domain structure was clearly detected under the polarizing microscope. Immediately after switching off a low-frequency square wave voltage, a typical stripe texture, running perpendicular to the rubbing direction, was observed, before the return of the ferroelectric helix took part. Dielectric spectroscopy clearly detects the domain mode relaxation. Figure 4(a), shows the imaginary part ($\varepsilon_\perp''$) of the dielectric permittivity versus the frequency at different temperatures in the Sm-C^* phase when the applied bias voltage is around 20 V (i.e., the helix is unwound). A typical Cole-Cole plot is shown in Fig. 4(b) for the domain mode process. As seen in Fig. 4(a) the position of the absorption peak is more or less independent of temperature, and if one looks carefully at the shoulder of the absorption curves (the higher-frequency side) there is a hump, suggesting that we are dealing here with two dielectric processes. The other absorption is due to the soft mode (fluctuations in the magnitude of the tilt of the molecules), which will be discussed in detail in Sec. III B. As seen in the figure the dielectric spectrum is rather complex. The dielectric parameters were computed by fitting a sum of two Cole-Cole functions:

$$\varepsilon_\perp^* = \varepsilon_\perp' - i\varepsilon_\perp'' = \varepsilon_{\perp\infty} + \frac{\Delta\varepsilon_D}{1+(i\omega\tau_D)^{1-\alpha_D}} + \frac{\Delta\varepsilon_S}{1+(i\omega\tau_S)^{1-\alpha_S}}\ , \tag{6}$$

which gives the best fits to the experimental points. Here $\Delta\varepsilon_D$ and $\Delta\varepsilon_S$ are the dielectric increments due to domain and soft mode relaxations, and α_D and α_S are the respective distribution parameters. Table I gives the different dielectric parameters of the domain mode. As seen in the table the relaxation frequency of the mode is almost independent of temperature, whereas the dielectric strength decreases with the increase in temperature. The detailed dynamics of the domain mode process are reported elsewhere [12,13].

3. *Soft mode in N^* and Sm-C^* phases*

The soft mode, which comes from fluctuations of the magnitude of the polarization vector, is well studied [1,14,15] in the second order phase transition FLC's in Sm-A and Sm-C^* phases, whereas in first order phase transition FLC's, possessing an N^* to Sm-C^* phase sequence, this effect has been scarcely studied [16,17], due first to the difficulty in alignment and second to the absence of the Sm-A phase. Moreover, there has been always doubt whether the electroclinic effect (soft mode) is due to the surface action or material property [18]. Therefore, in the present investigations, to minimize the surface effect, no surface treatment was done for aligning the FLC molecules, and the alignment was done by magnetic field. The soft mode is very clearly seen up to 5 K above the transition temperature in the N^* phase, as shown in Fig. 5. The absorption spectra show a single relaxation process and can be described by Eq. (4). The dielectric parameters for the soft mode process in the N^* phase are obtained by fitting a Cole-Cole function to the experimental points and shown in Table II. As seen from the Table, the relaxation frequency and dielectric increment of the soft mode is strongly temperature dependent. As one goes away from the T_c temperature in the N^* phase, the dielectric strength of soft mode becomes very weak and could not be detected.

The soft mode process has also been detected in the Sm-C^* phase, the only difference is that it is seen when a strong bias voltage of 30 V is applied to suppress the Goldstone mode. As was discussed earlier for strong bias voltages, the domain mode is also seen in the Sm-C^* phase. However, the relaxation frequencies of these two modes are well separated, and one can distinguish between the two. As we have seen in Fig. 4(a), in the Sm-C^* phase there is a dispersion region above the 100-kHz frequency, connected with the soft mode. However, if one magnifies the ε'' scale below the T_c temperature, a new relaxation region shows up, but its dispersion takes place at much higher frequencies in comparison to the domain mode as seen in Fig. 6. It is clear from the figure that as one goes away from the T_c temperature in the Sm-C^* phase, the absorption due to the soft mode decreases and the domain mode increases. Figure 7(a) shows a typical Cole-Cole plot for the soft mode in the N^* phase, showing that there is a single relaxation process. Figure 7(b) depicts the Cole-Cole plot in the Sm-C^* phase, suggesting very clearly two relaxation processes due to the soft mode and the domain mode that are quite well separated from each other. Two Cole-Cole functions [Eq. (6)] were fitted to the experimental points to calculate the dielectric parameters of the soft mode in the Sm-C^* phase and shown in Table II. As seen in the table the relaxation frequency of the soft mode is strongly temperature dependent very close to the T_c temperature

TABLE II. Dielectric parameters of the soft mode in two phases.

t (°C)	$\Delta\varepsilon_S$	ν_C^S (kHz)	α_S
	Sm-C^*		
37.63	0.16	1233.1	0.541
39.62	0.17	1024.5	0.296
41.64	0.22	983.6	0.432
43.65	0.51	1222.3	0.369
45.52	0.75	798.5	0.131
45.79	1.21	432.3	0.022
46.01	1.30	311.4	0.016
46.33	1.50	255.5	0.028
46.48	1.75	250.6	0.034
	N^*		
46.81	2.28	449.3	0.052
47.24	1.70	586.9	0.044
47.71	1.24	739.2	0.038
48.17	1.02	894.8	0.038
48.45	0.85	1115.2	0.030
49.43	0.59	1537.3	0.038
50.41	0.41	2021.4	0.054
51.30	0.29	2605.9	0.101
52.37	0.22	3117.4	0.082
53.37	0.13	5279.8	0.169

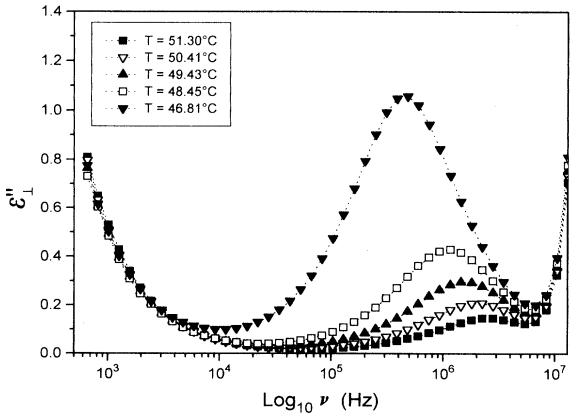

FIG. 5. Absorption curves for soft mode at different temperatures in the N^* phase (dotted lines are the fitting curves).

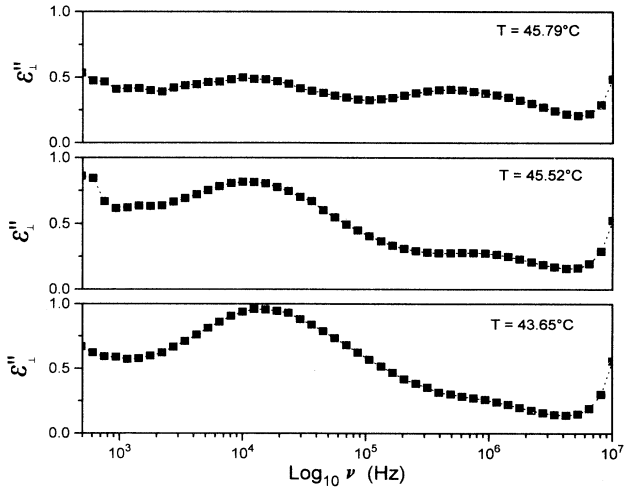

FIG. 6. Dielectric spectra (absorption curves) for soft mode and domain mode in the Sm-C^* phase for three temperatures close to the transition temperature. The spectra were obtained at 30-V biasing.

whereas deep in the Sm-C^* phase it is almost independent of temperature.

Figures 8(a) and 8(b) show the relaxation frequency and the inverse of dielectric ($\Delta\varepsilon_s^{-1}$) versus temperature of the soft mode very close to the transition temperature. It can be described with a typical V shape, which was predicted by theory [19]. It is clear from the figures and table that the soft mode obeys a Curie-Weiss law very close to the transition temperature which has been observed in a ferroelectric liquid crystal showing a first order phase transition, although this type of behavior is well established in second order phase transition FLCs [1,14,15]. However, deep in the Sm-C^* phase the relaxation frequency of the soft mode is almost independent of temperature (Table II), which has also been observed by Legrand *et al.* [20] in this type of FLC. Figure 8(c) shows the dielectric permittivity in planar alignment versus temperature very close to T_c at five different frequencies. As is seen, the dielectric permittivity distinctly increases at the transition temperature at frequencies of 56, 107, and 254 kHz, indicating that the soft mode is dominant close to the T_c temperature. It is worth mentioning here that the soft mode behavior near the transition temperature has also been checked in an ITO coated electrode cell where the planar alignment was perfect. The alignment in such cells were done by applying an electric field, just below the transition temperature (T_c) [21], and simultaneously observing under the polarizing microscope.

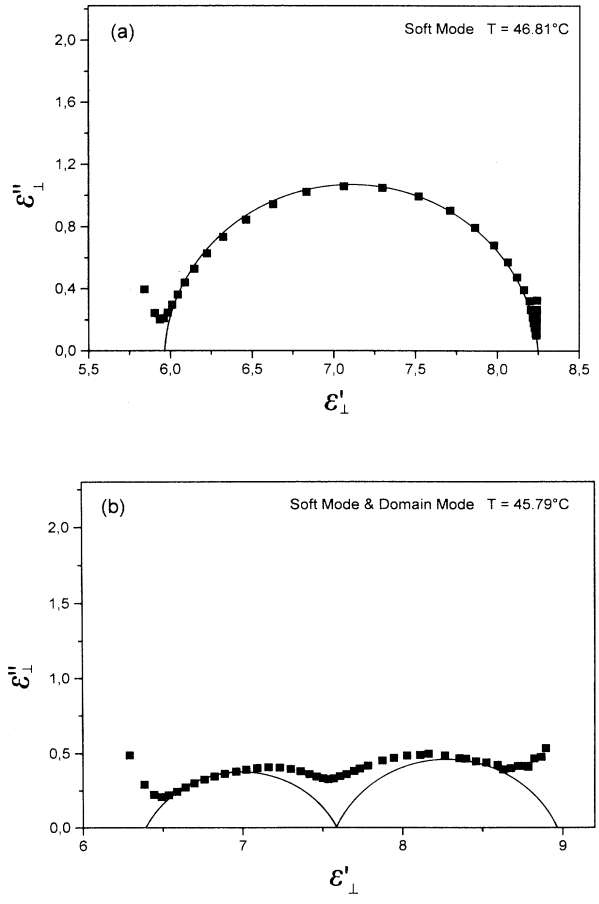

FIG. 7. (a) Cole-Cole plot for soft mode process in N^* phase. (b) Cole-Cole plot in the Sm-C^* phase, indicating soft mode (left hand side) and domain mode process (right hand side) which was obtained at the biasing of 30 V.

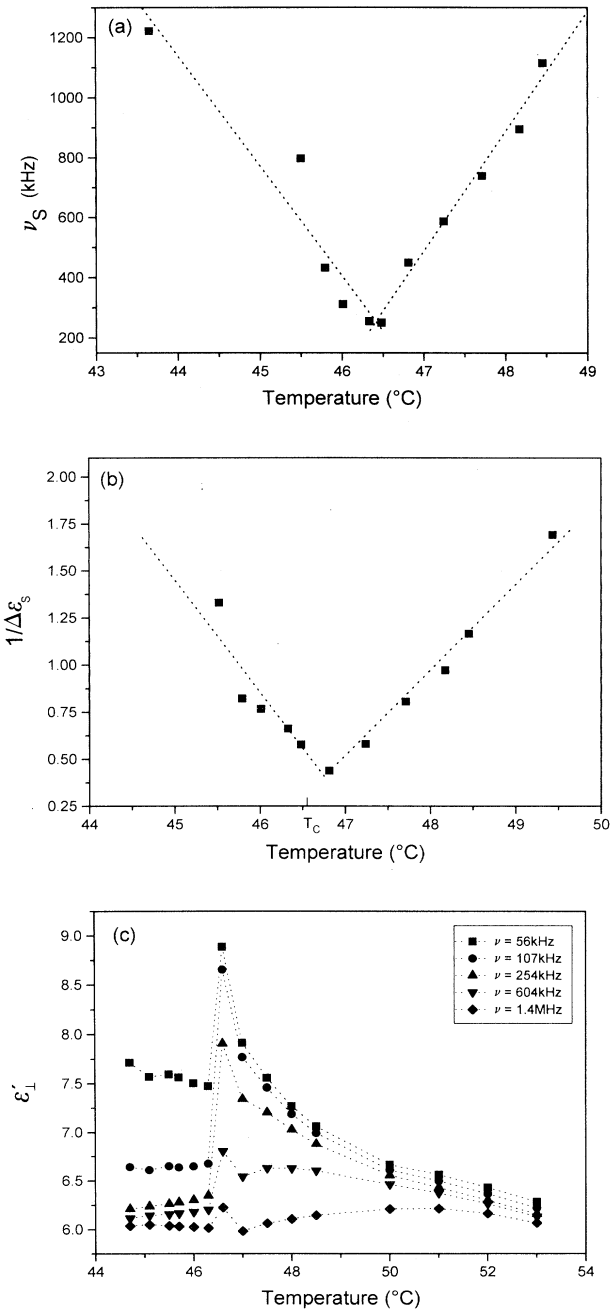

FIG. 8. (a) Temperature dependence of the relaxation frequency of the soft mode in Sm-C^* and N^* phases. (b) Inverse of dielectric strength vs temperature (Curie-Weiss plot) for the soft mode. (c) Dielectric permittivity ($\varepsilon'_\perp$) vs temperature at five different frequencies. All the plots were obtained close to the transition temperature of Sm-C^* to N^* phases.

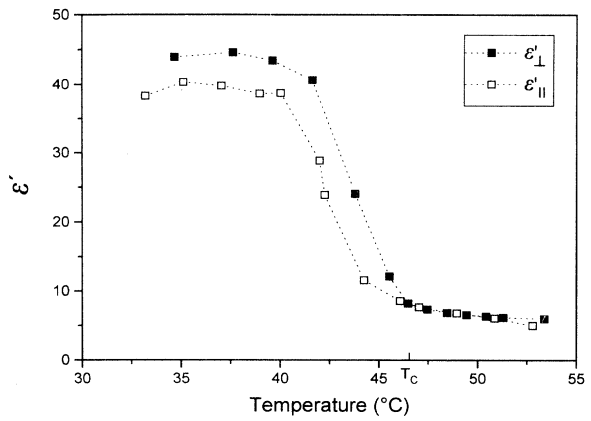

FIG. 9. Temperature dependences of two principal electric permittivities $\varepsilon'_\perp$ and $\varepsilon'_\parallel$ at 10-kHz frequency.

B. Dielectric anisotropy

Figure 9 shows the electric permittivity components in planar ($\varepsilon'_\perp$) and homeotropic ($\varepsilon'_\parallel$) alignment at 10-KHz frequency for different temperatures. As seen in the figure the dielectric permittivity for lower temperatures in the planar component ($\varepsilon'_\perp$) is very high, due to the Goldstone mode contribution in the Sm-C^* phase and because those other dielectric processes are not seen in the spectrum. In the homeotropic alignment ($\varepsilon'_\parallel$) the nature of the spectrum is almost the same, suggesting that the homeotropic alignment was not good. Moreover, when the FLC material is cooled down to the Sm-C^* phase the measuring electric field is no longer parallel to the director but it makes a wide angle (35° in this material) with the director, depending upon the tilt angle of the molecules [2], and hence the electric permittivity due to the $\varepsilon'_\perp$ (planar) component is dominant in homeotropic measurements (for the $\varepsilon'_\parallel$ component). This means that the dielectric processes in the planar component would also overlap in the homeotropic measurements.

C. $\varepsilon_\parallel$ component of the complex electric permittivity

Figure 10(a) shows the absorption spectrum in a homeotropically aligned (the $\varepsilon_\parallel$ component) cell in the chiral-nematic phase at different temperatures due to the rotation of the molecule around its short axis (a 180° jump around the short axis). The absorption spectra clearly show a single relaxation process of the Debye type, as also seen in the Cole-Cole plot [Fig. 10(b)]. How-

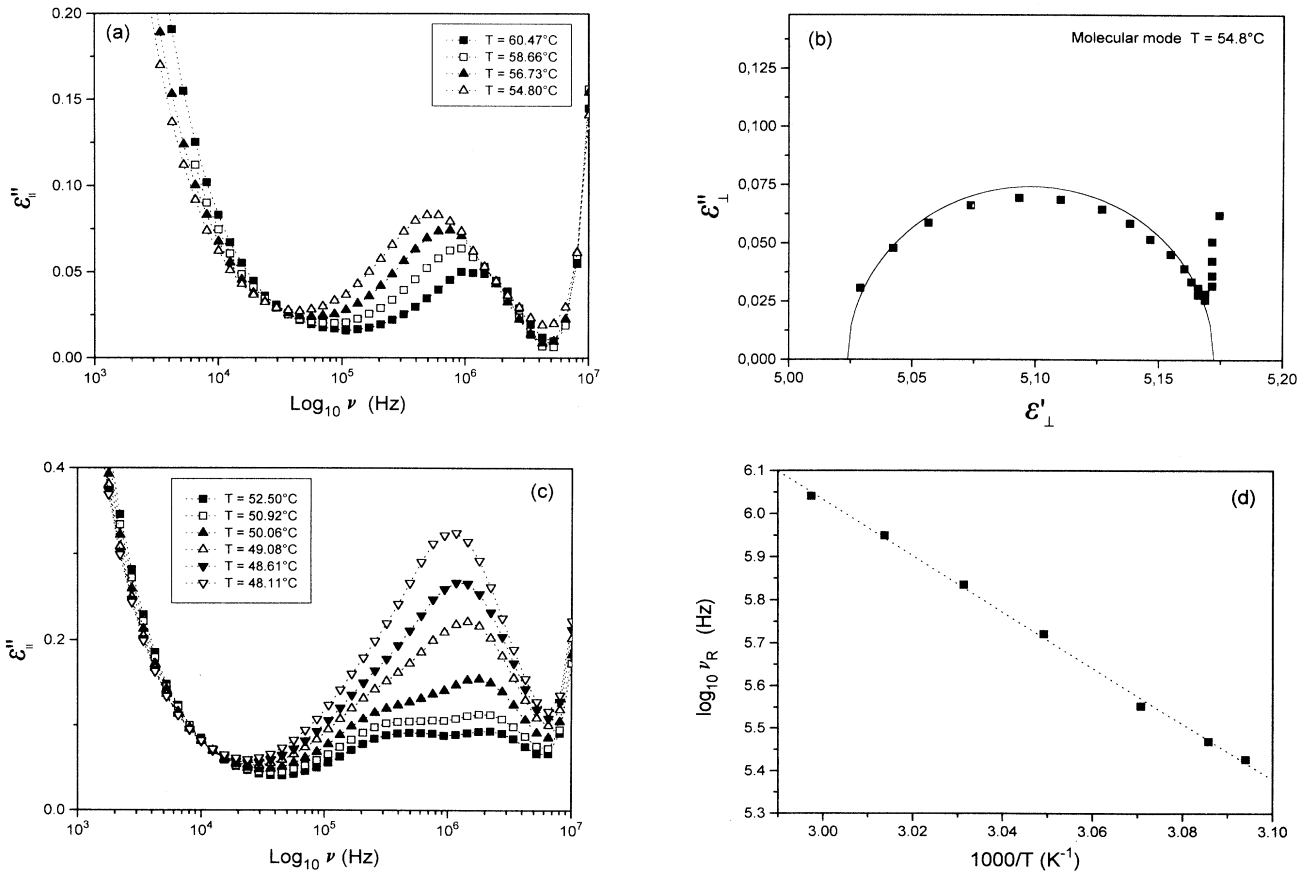

FIG. 10. (a) Absorption curves due to molecular relaxation around the short axis of the molecule in the N^* phase for different temperatures. (b) Cole-Cole plot for the molecular process. (c) Absorption curves due to molecular relaxation close to the transition temperature in the N^* phase for different temperatures (dotted lines are the fitting curves). (d) Arrhenius plot for the molecular process in the N^* phase.

TABLE III. Dielectric parameters of the molecular mode.

t (°C)	$\Delta\varepsilon_M$	ν_C^M (kHz)	α_M
50.06	0.166	267.6	0.042
50.92	0.153	294.6	0.033
52.50	0.144	357.5	0.091
54.80	0.143	526.1	0.018
56.73	0.148	684.4	0.009
58.66	0.120	891.2	0.002
60.47	0.088	1099.1	0.002

ever, close to the transition temperature the absorption peak is broadened, suggesting that there is more than one process, as seen in Fig. 10(c). At about 52.50 and 50.92 °C two processes, i.e., the molecular process and the soft mode process of the planar component, are clearly seen. Again, very close to the transition (below 50 °C) only one process is seen, which is due to the soft mode relaxation. It should be mentioned here that the absorption due to the molecular process is very weak, and the relaxation frequency falls in the same range of the soft mode very close to the transition temperature, and so it becomes very difficult to isolate the molecular process from the soft mode. The experimental points were fitted by Cole-Cole functions, and the dielectric parameters gathered in Table III for the molecular relaxation around the short axis. As seen in the table the relaxation frequency of the molecular process is temperature dependent, and shows Arrhenius-type behavior [Fig. 10(d)] in the N^* phase. However, very close to the transition temperature and in the Sm-C^* phase this process could not be detected due to an overlapping of the planar component in homeotropic measurements which is also clearly reflected in the dielectric anisotropy (Fig. 9).

D. Relaxation frequencies of different dielectric modes

Temperature dependences of the relaxation frequencies for different dielectric processes in planar and homeotropically aligned cells are depicted in Fig. 11 in the first order phase transition FLC material having a high-spontaneous-polarization value. As seen in the figure the soft mode is observed in N^* and Sm-C^* phases. The relaxation frequency is strongly temperature dependent very close to the transition temperature, and it obeys the Curie-Weiss law. Well below the T_c temperature in the Sm-C^* phase it is almost independent of temperature. Relaxation frequency of the Goldstone mode and the domain mode are almost independent of temperature in the Sm-C^* phase. As seen in the figure the relaxation frequency of the molecular process around the short axis of the molecule in homeotropic alignment is temperature dependent. The activation energy calculated for the molecular process is about 55 kJ/mol in the N^* phase, which is the typical value for the nematic phase.

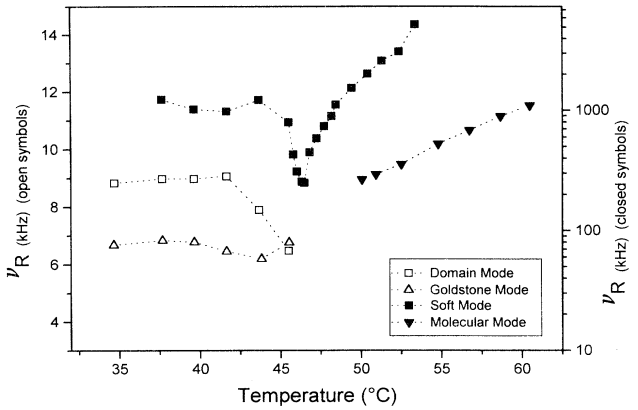

FIG. 11. Temperature dependences of the relaxation frequencies of the different dielectric modes in Sm-C^* and N^* phases in the planar and homeotropic alignment.

IV. CONCLUSIONS

(i) The soft mode dielectric process has been observed in the Sm-C^* and N^* phases. The relaxation frequency of the soft mode, very close to the transition temperature, fulfills the Curie-Weiss law which was observed in a first order phase transition ferroelectric liquid crystal. However, deep in the Sm-C^* phase the relaxation frequency of the soft mode is almost independent of temperature, which was also observed by Legrand *et al.* [20].

(ii) Three collective dielectric processes—a Goldstone mode, a domain mode, and a soft mode—connected to the director reorientation have been observed in the Sm-C^* phase. The relaxation frequencies and dielectric strengths of these three modes were well separated from each other in the planar component of the complex electric permittivity.

(iii) In homeotropic alignment a low-frequency molecular relaxation around the short axis of the molecule (180°-flip molecular relaxation) has been observed in the N^* phase. The molecular process shows an Arrhenius-type behavior of the critical frequencies in the N^* phase. However, due to the overlapping of the planar component ($\varepsilon_\perp$), this process could not be detected close to the transition temperature in the N^* phase or in the Sm-C^* phase.

ACKNOWLEDGMENTS

The authors sincerely thank the E. Merck Co. for supplying the liquid crystal material (IS-4362). We are thankful to KFA Jülich and CSIR, New Dehli, for supporting this work under the project of the German-India bilateral cooperation programme. We (W.H. and S.H.) also thank the Deutsche Forschungsgemeinschaft for financial support.

[1] T. Carlsson, B. Zeks, C. Filipc, and A. Levstik, Phys. Rev. A **45**, 877 (1990).
[2] F. Gouda, G. Anderson, M. Matuszczyk, T. Matuszczyk, K. Skarp, and S. T. Lagerwall, J. Appl. Phys. **67**, 180 (1990).
[3] J. Pavel, M.Glogarova, and S. S. Bawa, Ferroelectrics **76**, 221 (1987).
[4] A. M. Biradar, S. Wrobel, and W. Haase, Phys. Rev. A **39**, 2693 (1989).
[5] A. M. Biradar, S. S. Bawa, and Subhas Chandra, Phys. Rev. A **45**, 7282 (1992).
[6] A. M. Biradar, S. S. Bawa, C. P. Sharma, and Subhas Chandra, Ferroelectrics **122**, 81 (1991).
[7] K. Kondo, T. Kitamura, M. Isogai, and A. Mukoh, Ferroelectrics **132**, 99 (1988).
[8] L. A. Beresnev, M. Pfeiffer, S. A. Pikin, W. Haase, and L. M. Blinov, Ferroelectrics **132**, 99 (1992).
[9] L. Benguigui, J. Phys. (Paris) **43**, 912 (1982).
[10] W. Haase, H. Pranoto, and F. J. Bormuth, Ber. Bunsenges. Phys. Chem. **89**, 1229 (1985).
[11] S. Wrobel, M. Marzec, M. Godlewska, B. Gestblom, S. Hiller, and W. Haase, Proc. SPIE **2372**, 169 (1995).
[12] S. A. Pikin, L. A. Beresnev, S. Hiller, M. Pfeiffer, and W. Haase, Mol. Mater. **3**, 1 (1993); W. Haase, S. Hiller, M. Pfeiffer, and L. A. Beresnev, Ferroelectrics **140**, 37 (1993).
[13] L. A. Beresnev, E. Schumacher, S. A. Pikin, Z. Fan, B. I. Ostrovsky, S. Hiller, A. P. Onokhov, and W. Haase, Jpn. J. Appl. Phys. **34**, 2404 (1995).
[14] F. Gouda, G. Andersson, T. Carlsson, S. T. Lagerwall, K. Skarp, B. Stebler, C. Filipic, B. Zeks, and A. Levstik, Mol. Cryst. Liq. Cryst. Lett. **6**, 151 (1988).
[15] S. Wrobel, A. M. Biradar, and W. Haase, Ferroelectrics **100**, 271 (1989).
[16] A. M. Biradar, S. S. Bawa, K. Saxena, and Subhas Chandra, J. Phys. II (France) **3**, 1787 (1993).
[17] Z. Li, R. G. Petschek, and C. Rosenblatt, Phys. Rev. Lett. **62**, 796 (1989).
[18] L. Komitov, S. T. Lagerwall, B. Stebler, G. Andersson, and K. Flatichler, Ferroelectrics **114**, 167 (1991).
[19] R. Blinc and B. Zeks, Phys. Rev. A **18**, 741 (1978).
[20] C. Legrand, N. Isaert, J. Hmine, J. M. Buisine, J. P. Parneix, H. T. Nguyen, and C. Destrade, Ferroelectrics **121**, 21 (1991).
[21] J. S. Patel and J. W. Goodby, J. Appl. Phys. **59**, 2355 (1986).